National Conference with International Participations

ENGINEERING MECHANICS 2008

Svratka, Czech Republic, May 12 – 15, 2008

NUMERICAL EXPERIMENTS IN A GLOBAL ENERGETIC MODEL OF DAMAGE

J. Zeman*, T. Roubíček, A. Mielke*****

Summary: *This paper presents a Finite Element-based approach to constructing an approximate energetic solution to a non-local damage model proposed by Mielke and Roubíček (2006). Particular emphasis is given to obtaining a solution based on global rather that local energy minimization. Performance of the model and the numerical scheme is demonstrated on a basic two-dimensional example.*

1 Introduction

Damage presents an inelastic load-induced response of solid bodies, which is typical of quasi-brittle materials. Physically speaking, it is usually interpreted as a collective effect of microstructural failures, leading finally to the macroscopic collapse of the structure. Due to obvious reasons, the damage theories have received a great attention in the engineering literature and huge amount of theoretical, numerical and experimental work has been invested into understanding and prediction of damage processes, see e.g. (Jirásek and Bažant, 2002, Chapter 26) for a systematic discussion.

In this contribution, we present an overview of theoretical and numerical results related to a specific global (i.e. non-local) rate-independent isotropic damage model proposed by Mielke and Roubíček (2006), which is inspired by an engineering damage model due to Frémond and Nedjar (1996). Unlike its engineering counterpart, however, the former approach is supported by a number of rigorous mathematical results (Mielke and Roubíček, 2006; Bouchitté et al., 2007; Mielke et al., 2007) as well as a simple bifurcation study (Jirásek and Zeman, 2008).

The rest of the paper is organized as follows. Section 2 briefly overviews the essential components of the adopted modeling framework and its application to the damage modeling. In addition, an abstract approximation result is presented to prepare the footing for the subsequent numerical treatment. Section 3 presents the fully discrete version of the problem together with its efficient numerical solution. In addition, a simple backtracking-in-time procedure is proposed to obtain results consistent with the requirements of the underlying theory. Finally, Section 4 demonstrates the theoretical principles on a simple uniaxial tension experiment.

*Ing. Jan Zeman, Ph.D.: Department of Mechanics, Faculty of Civil Engineering, Czech Technical University in Prague, Thákurova 7; 166 29 Prague 6; tel.: +420-2-2435-4482, fax: +420-2-2431-0775; e-mail: zemanj@cml.fsv.cvut.cz

**Prof. Ing. Tomáš Roubíček, DrSc.: Mathematical Institute, Charles University; Sokolovská 83; 186 75 Praha 8-Karlín; Institute of Information Theory and Automation, Academy of Sciences of the Czech Republic; Pod vodárenskou věží 4, 182 08 Praha 8-Kobylisy Sokolovská 83; 186 75 Praha 8-Karlín tel. +420-2-2191-3213:, fax: +420-2-2232-3394; e-mail: tomas.roubicek@mff.cuni.cz

***Prof. Dr. Alexander Mielke: Weierstrass Institute for Applied Analysis and Stochastics; Mohrenstrasse 39; 10117 Berlin; Department of Mathematics, Humboldt University of Berlin; Rudower Chaussee 25, 12489 Berlin tel.: ++49-30-20372-563, fax: +49-30-2044975; e-mail: mielke@wias-berlin.de

2 Methods

2.1 Global energetic formulation

Let us consider a damaging body subject to displacement-controlled loading program. In the sequel, the body will be represented by a set $\Omega \subset \mathbb{R}^d$ with boundary Γ, subjected to the Dirichlet loading Γ_{D}. Symbol t denotes the (pseudo-) time taken from interval $I = [0; T]$.

Following the standard thermodynamic approach to constitutive modeling, cf. (Jirásek and Bažant, 2002, Chapter 25), a state of the system is described using an admissible displacement and internal variables $\widehat{\boldsymbol{u}}$ and $\widehat{\zeta}$, respectively. Formally, we write

$$\widehat{\boldsymbol{u}} : \Omega \to \mathbb{R}^d, \widehat{\boldsymbol{u}} \in \mathbb{K} \qquad \widehat{\zeta} : \Omega \to \mathbb{R}, \widehat{\zeta} \in \mathbb{Z} \tag{1}$$

where where $\mathbb{K}$ denotes the set of kinematically admissible displacements and $\mathbb{Z}$ stands for the set of admissible internal variables.

Within the adopted *global* energetic framework (Mielke, 2005), the constitutive description of the damage model is provided by the *stored energy* functional

$$\mathcal{E}(t, \widehat{\boldsymbol{u}}, \widehat{\zeta}) : I \times \mathbb{K} \times \mathbb{Z} \to \mathbb{R} \tag{2}$$

and by the *dissipation distance*

$$\mathcal{D}(\widehat{\zeta}^1, \widehat{\zeta}^2) : \mathbb{Z} \times \mathbb{Z} \to \mathbb{R}. \tag{3}$$

Physically, $\mathcal{E}$ represents the energy reversibly stored in the system, whereas $\mathcal{D}$ is the energy dissipated by changing the field of internal variables from $\widehat{\zeta}^1$ to $\widehat{\zeta}^2$. The last component of the model is given by specifying the power of external loading

$$\mathcal{P}(t, \widehat{\boldsymbol{u}}, \widehat{\zeta}) : \mathbb{K} \times \mathbb{Z} \to \mathbb{R}. \tag{4}$$

Now, given the loading term $\mathcal{P}$, energetic functionals $\mathcal{E}$ and $\mathcal{D}$ and initial data $\boldsymbol{u}(0)$ and $\zeta(0)$, the *energetic solution* of the rate-independent evolution is provided by functions $\boldsymbol{u}(t)$ and $\zeta(t)$ satisfying (Mielke, 2005):

Global stability: for all $t \in (0; T]$, $\widehat{\boldsymbol{u}} \in \mathbb{K}$ and $\widehat{\zeta} \in \mathbb{Z}$

$$\mathcal{E}\left(t, \boldsymbol{u}(t), \zeta(t)\right) \leq \mathcal{E}(t, \widehat{\boldsymbol{u}}, \widehat{\zeta}) + \mathcal{D}(\zeta(t), \widehat{\zeta}) \tag{5}$$

Energy balance: for all $t \in (0; T]$

$$\mathcal{E}(t, \boldsymbol{u}(t), \zeta(t)) + \mathrm{Var}_{\mathcal{D}}(\zeta(t), [0, t]) = \mathcal{E}(0, \boldsymbol{u}(0), \zeta(0)) + \int_0^t \mathcal{P}(s, \boldsymbol{u}(s), \zeta(s))\, \mathrm{d}s, \tag{6}$$

where $\mathrm{Var}_{\mathcal{D}}$ quantifies totally dissipated energy by the process ζ during time interval $[0, t]$.

2.2 Application to damage

The previously introduced framework can be readily applied to the problem of damage, cf. (Mielke and Roubíček, 2006; Bouchitté et al., 2007). In particular, in order to accommodate the time-dependent Dirichlet loading, corresponding to a displacement-controlled experiment, we consider (with a slight abuse on notation) a split of the displacement field in the from

$\boldsymbol{u}_{\mathrm{D}}(t) + \widehat{\boldsymbol{u}}$, where $\boldsymbol{u}_{\mathrm{D}}$ is an appropriate extension of the prescribed Dirichlet boundary data and the set of kinematically admissible displacements is defined as

$$\mathbb{K} = \left\{ \widehat{\boldsymbol{u}} \in W^{1,2}(\Omega; \mathbb{R}^d), \widehat{\boldsymbol{u}}|_{\Gamma_{\mathrm{D}}} = \boldsymbol{0} \right\}, \tag{7}$$

where $W^{1,2}$ is the Sobolev space of functions with square-integrable weak derivatives, see e.g. (Roubíček, 2005). Moreover, the interval variable $\widehat{\zeta}$ has now the physical meaning of the *integrity field*,[1] constrained to an admissible set

$$\mathbb{Z} = \left\{ \widehat{\zeta} \in W^{1,2}(\Omega; \mathbb{R}), 0 \leq \widehat{\zeta}(x) \leq 1 \text{ a.e. in } \Omega \right\}. \tag{8}$$

The stored energy is assumed in the form

$$\mathcal{E}^{\epsilon}(t, \widehat{\boldsymbol{u}}, \widehat{\zeta}) = \int_{\Omega} \frac{\epsilon + \widehat{\zeta}}{2} \boldsymbol{\varepsilon}(\widehat{\boldsymbol{u}} + \boldsymbol{u}_{\mathrm{D}}(t)) : \boldsymbol{C} : \boldsymbol{\varepsilon}(\widehat{\boldsymbol{u}} + \boldsymbol{u}_{\mathrm{D}}(t)) + \frac{1}{2}\kappa \left| \nabla \widehat{\zeta} \right|^2 \mathrm{d}\Omega, \tag{9}$$

where $\boldsymbol{\varepsilon}(\widehat{\boldsymbol{u}})$ is the linearized strain corresponding to a displacement field $\widehat{\boldsymbol{u}}$, $\boldsymbol{C}$ is a fourth-order tensor of elastic stiffness, κ is an influence factor introducing an internal length into the formulation and ϵ is a regularization parameter, related to the residual stiffness corresponding to "complete damage" ($\widehat{\zeta} = 0$). The dissipation distance is expressed as

$$\mathcal{D}(\widehat{\zeta}^1, \widehat{\zeta}^2) = \begin{cases} \displaystyle\int_{\Omega} a(\boldsymbol{x}) \left(\widehat{\zeta}^1(\boldsymbol{x}) - \widehat{\zeta}^2(\boldsymbol{x}) \right) \mathrm{d}\boldsymbol{x} & \text{if } \widehat{\zeta}^1 \geq \widehat{\zeta}^2 \text{ a.e.} \\ +\infty & \text{otherwise} \end{cases} \tag{10}$$

with a denoting an activation threshold (related to strength of a material) and the term "$+\infty$" ensures the irreversibility of the damage evolution; i.e. at any point, the integrity variable cannot increase in time. Finally, the power of external forces is given by

$$\mathcal{P}^{\epsilon}(t, \widehat{\boldsymbol{u}}, \widehat{\zeta}) = \int_{\Omega} \boldsymbol{\varepsilon} \left(\frac{\partial \boldsymbol{u}_{\mathrm{D}}(t)}{\partial t} \right) : \boldsymbol{\sigma}^{\epsilon}(t, \widehat{\boldsymbol{u}}, \widehat{\zeta}) \, \mathrm{d}\boldsymbol{x} \tag{11}$$

where the ϵ-regularized stress $\boldsymbol{\sigma}^{\epsilon}$ provided by

$$\boldsymbol{\sigma}^{\epsilon}(t, \widehat{\boldsymbol{u}}, \widehat{\zeta}) = (\widehat{\zeta} + \epsilon) \boldsymbol{C} : \boldsymbol{\varepsilon}(\widehat{\boldsymbol{u}} + \boldsymbol{u}_{\mathrm{D}}(t)) \tag{12}$$

2.3 Time-incremental formulation

Although the previously mentioned conditions (5) and (6) present the formal definition of the energetic solution, the analysis itself will be performed using the time discretization technique, see e.g. (Rektorys, 1982) for a nice exposition. To that end, we introduce a uniform partitioning of the time interval $0 = t_0 < t_1 = t_0 + \tau < \ldots < t_N = T$ and inductively solve the minimization problem

$$(\boldsymbol{u}_k, t_k) \in \operatorname{Arg} \min_{(\widehat{\boldsymbol{u}}, \widehat{\zeta}) \in \mathbb{K} \times \mathbb{Z}} \left[\mathcal{E}(t_k, \widehat{\boldsymbol{u}}, \widehat{\zeta}) + \mathcal{D}(\zeta(t_{k-1}), \widehat{\zeta}) \right] \text{ for } k = 1, 2, \ldots, N \tag{13}$$

Note that the previous problem is independent from τ, which is consistent with the assumed rate-independent character of the damage process. The theoretical results gathered in (Mielke

[1] Note that in engineering models of damage, the *damage* variable $\omega = 1 - \zeta$ is usually employed.

and Roubíček, 2006; Bouchitté et al., 2007; Mielke et al., 2007) show that, under reasonable data qualification, the solution of the time-discretized problem converges to the energetic solution as $\tau \to 0$. Moreover, at each time step, the energetic solution verifies the two-sided energy inequality:

$$\begin{aligned} \int_{t_{k-1}}^{t_k} \mathcal{P}^\epsilon(s, \boldsymbol{u}_k, \zeta_k)\,\mathrm{d}s &\leq \mathcal{E}^\epsilon(t_k, \boldsymbol{u}_k, \zeta_k) - \mathcal{E}^\epsilon(t_{k-1}, \boldsymbol{u}_{k-1}, \zeta_{k-1}) + \mathcal{D}(\zeta_{k-1}, \zeta_k) \\ &\leq \int_{t_{k-1}}^{t_k} \mathcal{P}^\epsilon(s, \boldsymbol{u}_{k-1}, \zeta_{k-1})\,\mathrm{d}s \end{aligned} \tag{14}$$

2.4 Abstract approximation result

The last step of the theoretical setup is conversion of the previous semi-discretized problem into a fully discrete one. To that end, consider finite-dimensional subspaces

$$\mathbb{K}_h \subset \mathbb{K} \quad \text{and} \quad \mathbb{Z}_h \subset \mathbb{Z}.$$

Executing the incremental minimization, recall Eq. (13), with $\mathbb{K}$ and $\mathbb{Z}$ replaced with the discrete counterparts yields the *approximate* energetic solution $(\boldsymbol{u}^\epsilon_{\tau h}, \zeta^\epsilon_{\tau h})$.

As shown by Mielke and Roubíček (2006), the convergence of the approximate solution to the time-continuous one, i.e. as $\tau \to 0$ and $h \to 0$, requires[2]

Energetic density of $\mathbb{K}_h \times \mathbb{Z}_h$: For all $t \in I$ and $(\widehat{\boldsymbol{u}}, \widehat{\zeta}) \in \mathbb{K} \times \mathbb{Z}$ with $\mathcal{E}^\epsilon(t, \widehat{\boldsymbol{u}}, \widehat{\zeta}) < \infty$, there exists $\{(\widehat{\boldsymbol{u}}_h, \widehat{\zeta}_h)\}_{h>0}$ such that $(\widehat{\boldsymbol{u}}_h, \widehat{\zeta}_h) \rightharpoonup (\widehat{\boldsymbol{u}}, \widehat{\zeta})$ and $\mathcal{E}^\epsilon(t, \widehat{\boldsymbol{u}}_h, \widehat{\zeta}_h) \to \mathcal{E}^\epsilon(t, \widehat{\boldsymbol{u}}, \widehat{\zeta})$.

In the current setting, this condition is met for a piecewise-linear discretization of the involved fields on simplicial meshes (Mielke and Roubíček, 2006), which opens the route to the implementation of numerical algorithm.

3 Numerics

3.1 Finite element discretization

Following the standard Finite Element procedures, e.g. (Bittnar and Šejnoha, 1996), the discretized version of the kinematics and integrity fields are provided with

$$\boldsymbol{u}^\epsilon_{kh}(\boldsymbol{x}) = \boldsymbol{N}^u_h(\boldsymbol{x})\boldsymbol{d}^u_{kh}, \qquad \zeta^\epsilon_{kh}(\boldsymbol{x}) = \boldsymbol{N}^\zeta_h(\boldsymbol{x})\boldsymbol{d}^\zeta_{kh}, \tag{15}$$

where $\boldsymbol{N}^u_h$ and $\boldsymbol{N}^\zeta_h(\boldsymbol{x})$ denote the matrix of basis functions, while $\boldsymbol{d}^u_{kh}$ and $\boldsymbol{d}^\zeta_{kh}$ are the associated nodal values related to the time level t_k. The discrete incremental minimization problem can now be recast in the form

$$\left.\begin{aligned} &\text{minimize} \quad \frac{1}{2}\left(\boldsymbol{d}^u_{kh} + \boldsymbol{d}^u_{\mathrm{D},h}(t_k)\right)^{\mathsf{T}} \boldsymbol{K}^u_h(\boldsymbol{\zeta}_{kh})\left(\boldsymbol{d}^u_{kh} + \boldsymbol{d}^u_{\mathrm{D},h}\right) + \frac{1}{2}\boldsymbol{d}^\zeta_{kh}{}^{\mathsf{T}} \boldsymbol{K}^\zeta_h \boldsymbol{d}^\zeta_{kh} + \boldsymbol{f}^{\mathsf{T}}_{kh}\boldsymbol{d}^\zeta_{kh} \\ &\text{subject to} \quad \boldsymbol{0} \leq \boldsymbol{d}^\zeta \leq \boldsymbol{d}^\zeta_{k-1h}, \quad \boldsymbol{d}^u_{kh,\mathrm{D}} = \boldsymbol{0} \end{aligned}\right\} \tag{16}$$

[2]Note that the symbol "$\rightharpoonup$" stands for the weak convergence, cf. (Rektorys, 1982; Roubíček, 2005).

with the individual matrices provided by (k is omitted for the sake of brevity)

$$\boldsymbol{K}_h^u\left(\boldsymbol{d}_h^\zeta\right) = \int_{\Omega_h} \boldsymbol{B}_h^{u\mathsf{T}}(\boldsymbol{x})\left(\left(\epsilon + \boldsymbol{N}_h^\zeta(\boldsymbol{x})\boldsymbol{d}_h^\zeta\right)\boldsymbol{C}(\boldsymbol{x})\right)\boldsymbol{B}_h^u(\boldsymbol{x})\,\mathrm{d}\boldsymbol{x}, \tag{17}$$

$$\boldsymbol{K}_h^\zeta = \int_{\Omega_h} \boldsymbol{B}_h^{\zeta\mathsf{T}}\kappa(\boldsymbol{x})\boldsymbol{B}_h^\zeta(\boldsymbol{x})\,\mathrm{d}\boldsymbol{x}, \tag{18}$$

$$\boldsymbol{f}_h^\zeta = -\int_{\Omega_h} a(\boldsymbol{x})\boldsymbol{N}_h^{\zeta\mathsf{T}}(\boldsymbol{x})\,\mathrm{d}\boldsymbol{x}. \tag{19}$$

Hence, in the discretized form, solution of Eq. (16) leads to a large-scale, sparse, non-convex and bound-constrained optimization problem.

3.2 Alternate minimization algorithm

As efficient way to the treatment of the previously introduced optimization problem is to exploit its sparsity and simple form of the constraints. Such an approach is offered by the *alternate minimization algorithm* recently proposed in (Bourdin, 2007; Bourdin et al., 2008), which is similar to the operator split procedures of computational mechanics, cf. (Ortiz and Simo, 1986). The basic principle of the algorithm is illustrated in Table 1:

1: Set $j = 0$
2: **repeat**
3: Set $j = j + 1$
4: Solve $\boldsymbol{d}^{u(j)} = \arg\min \frac{1}{2}\left(\boldsymbol{d}^u + \boldsymbol{d}_{\mathrm{D},h}^u\right)^{\mathsf{T}} \boldsymbol{K}_h^u(\boldsymbol{d}^{\zeta(j-1)})\left(\boldsymbol{d}^u + \boldsymbol{d}_{\mathrm{D},h}^u\right)$
5: Solve $\boldsymbol{d}^{\zeta(j)} = \arg \min_{\mathbf{0}\le\boldsymbol{d}^\zeta\le\boldsymbol{d}_{k-1h}^\zeta} \frac{1}{2}\boldsymbol{d}^{u(j)\mathsf{T}}\boldsymbol{K}_h^u(\boldsymbol{d}^{\zeta(j-1)})\boldsymbol{d}^{u(j)} + \frac{1}{2}\boldsymbol{d}^{\zeta\mathsf{T}}\boldsymbol{K}_h^\zeta\boldsymbol{d}^\zeta + \boldsymbol{f}_h^{\zeta\mathsf{T}}\boldsymbol{d}^\zeta$
6: **until** $\|\boldsymbol{d}^{\zeta(j)} - \boldsymbol{d}^{\zeta(j-1)}\|_\infty \le \delta$
7: Set $\boldsymbol{d}_{kh}^u = \boldsymbol{d}^{u(j)}$, $\boldsymbol{d}_{kh}^\zeta = \boldsymbol{d}^{\zeta(j)}$

Table 1: Conceptual implementation of Alternate minimization algorithm

Convergence properties of the algorithm were studied in (Bourdin, 2007), where the convergence of the algorithm to a *critical* point of the objective function was demonstrated.

3.3 Backtracking procedure

Of course, there is no guarantee that the critical point is a global minimizer of the non-convex objective function, which is a crucial assumption of the theoretical framework. In the current work, the "globalization" of the alternate minimization procedure is performed using the two-sided energetic estimate Eq. (14), checked with a tolerance η to account for the discretization errors.

In particular, if the result of the alternate minimization algorithm fails to verify the inequality Eq. (14), the algorithm is restarted from the previous time level with $\boldsymbol{d}_{kh}^\zeta$ used as an initial guess for the minimization algorithm instead of $\boldsymbol{d}_{k-1h}^\zeta$. This procedure is repeated until an admissible solution is found, see Table 2 for additional details.

1	:	Set $k = 1$, $\boldsymbol{d}^{\zeta}_{-1h} = \mathbf{0}$, $\boldsymbol{d}^{\zeta}_{0h} = \mathbf{0}$, $\boldsymbol{d}^{\zeta^{(0)}} = \mathbf{0}$
2	:	**repeat**
3	:	Determine $\boldsymbol{d}^{\zeta}_{kh}$ using the alternate minimization algorithm for time t_k and initial value $\boldsymbol{d}^{\zeta^{(0)}}$.
4	:	Set $\boldsymbol{d}^{\zeta^{(0)}} = \boldsymbol{d}^{\zeta}_{kh}$
5	:	**if** two-sided inequality is satisfied with tolerance η
6	:	Set $k = k + 1$
7	:	**else**
8	:	Set $k = k - 1$
9	:	**end**
10	:	**until** $k \leq N$

Table 2: Conceptual implementation of backtracking algorithm

4 Illustrative example

Performance of the proposed algorithm will be illustrated on a "standard" benchmark problem: a uniaxial tension specimen with an initial imperfection, see Figure 1.

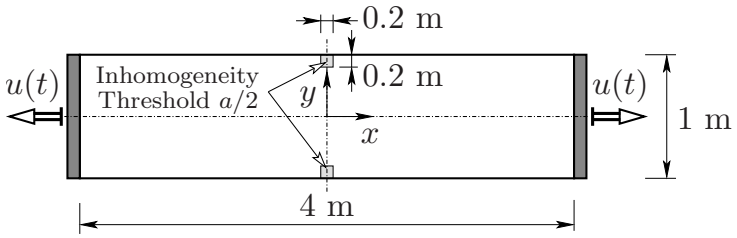

Figure 1: Experiment setup

The corresponding geometric and material data together with the algorithm parameters are gathered in Figure 1 and Table 3, respectively. The structure is assumed to be in the plane stress state and are subject to a proportional-in-time hard-device loading. The spatial discretization was performed using the unstructured mesh generator T3D (Rypl, 1998) and the problem size was reduced using symmetries of the specimens. The bound-constrained optimization problem was solved using a reflective Newton method (Coleman and Li, 1996), implemented in MATLAB®. The analyzed time interval $[0, 1]$ was decomposed into 100 identical time steps.

Young's modulus, E	27 GPa
Possion's ratio, ν	0.2
Factor of influence, κ	10 Jm^{-2}
Activation threshold, a	500 Jm^{-3}
Maximal prescribed displacement	$5 \cdot 10^{-4}$ m
Time step, τ	0.01
Damage profile tolerance, δ	10^{-6}
Two-sided energy inequality tolerance, η	10^{-3}

Table 3: Parameters of the damage model and incremental algorithm

The resulting energetics for the analyzed specimen is displayed in Figure 2 for a representa-

tive choice of the ϵ and h parameters. Clearly, in its basic version, the discrete solution obtained by the alternate minimization algorithm fails to provide an appropriate energetic solution to the problem. The two-sided inequality is satisfied only in the initial stage, where the specimen stays mainly elastic. At time $t \approx 0.61$, the damage propagates simultaneously through the specimen, as manifested by the drop of the sum of the globally dissipated and the reversibly energy, see Figure 2(a). Even after this instant, however, this quantity increases, which is the consequence of the non-zero value of regularization parameter ϵ. Moreover, the damage profile still evolves in the subsequent time levels, leading to the increase in the dissipated energy balanced by the contribution of the stored energy.

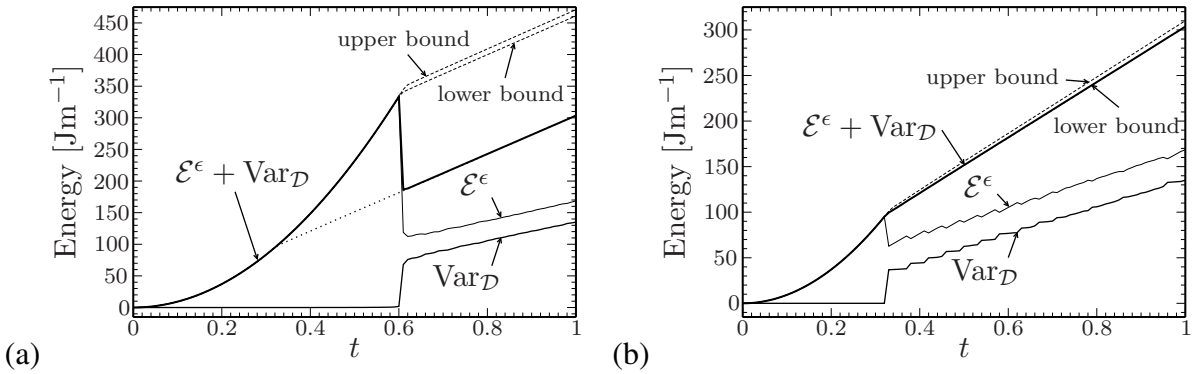

Figure 2: Energetics of the damage process; (a) without backtracking, (b) with backtracking.

With the backtracking option active, however, the algorithm detects the local minimizer at $t \approx 0.61$ and, following the dotted line in Figure 2(a), returns to the time level where the incremental two-sided inequality is satisfied. After the backtracking stage is completed, the alternate minimization algorithm is capable of finding an approximate energetic solution, cf. Figure 2(b).

Additional numerical tests summarized in Figure 3 demonstrate the "mesh-independent" behavior of the method, i.e. the fact that the global energetic response is almost independent of the discretization parameter h. The influence of the energy regularization parameter ϵ, however, is much stronger, cf. Figure 3(b). In particular, it can be observed that, as $\epsilon \to 0$, the algorithms tries to reproduce an one-dimensional damage profile studied in detail by Jirásek and Zeman (2008).

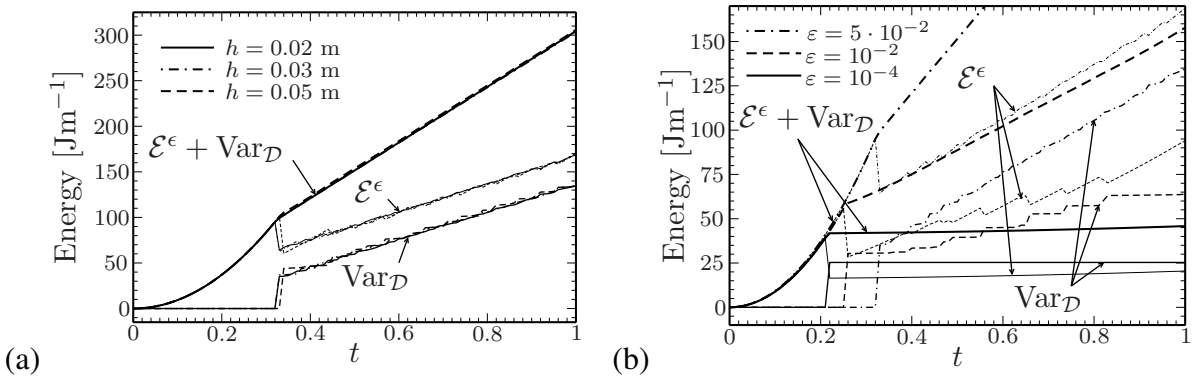

Figure 3: Convergence of the approximate energetic solution for the inhomogeneous specimen; (a) $h \to 0$ m, $\varepsilon = 5{\cdot}10^{-2}$, (b) $\varepsilon \to 0$, $h = 0.02$ m; mesh with $h = 0.05$ m contains 493 triangular elements, $h = 0.03$ m corresponds to $1,193$ elements and $h = 0.02$ m to $1,549$ elements.

An interested reader is referred to (Mielke et al., 2007) for further details and numerical examples.

Acknowledgment Financial support from the grant No. 106/08/1379 (GAČR) is gratefully acknowledged.

References

Bittnar, Z. and Šejnoha, J. (1996). *Numerical methods in structural mechanics*. ASCE Press and Thomas Telford, Ltd, New York and London.

Bouchitté, G., Mielke, A., and Roubíček, T. (2007). A complete-damage problem at small strains. *Zeitschrift für Angewandte Mathematik und Physik (ZAMP)*. Online first, http://dx.doi.org/10.1007/00033-007-7064-0.

Bourdin, B. (2007). Numerical implementation of the variational formulation of brittle fracture. *Interfaces and Free Boundaries*, 9(3):411–430.

Bourdin, B., Francfort, G., and Marigo, J.-J. (2008). The variational approach to fracture. *Journal of Elasticity*, 91(1):5–148.

Coleman, T. and Li, Y. (1996). A reflective newton method for minimizing a quadratic function subject to bounds on some of the variables. *SIAM Journal on Optimization*, 6(4):1040–1058.

Frémond, M. and Nedjar, B. (1996). Damage, gradient of damage and principle of virtual power. *International Journal of Solids and Structures*, 33(8):1083–1103.

Jirásek, M. and Bažant, Z. (2002). *Inelastic Analysis of Structures*. John Wiley & Sons, Chichester, England.

Jirásek, M. and Zeman, J. (2008). Localization study of a non-local energetic damage model. http://arxiv.org/abs/0804.3440.

Mielke, A. (2005). Evolution of rate-independent systems. In Dafermos, C. and Feireisl, E., editors, *Handbook of Differential Equations: Evolutionary Equations*, volume 2, pages 461–559. Elsevier B.V., Amsterdam, The Netherlands.

Mielke, A. and Roubíček, T. (2006). Numerical approaches to rate-independent processes and applications in inelasticity. WIAS Preprint 1169, Weierstrass Institute for Applied Analysis and Stochastics, Berlin.

Mielke, A. and Roubíček, T. (2006). Rate-independent damage processes in nonlinear elasticity. *Mathematical Models and Methods in Applied Sciences*, 16:177–209.

Mielke, A., Roubíček, T., and Zeman, J. (2007). Complete damage in elastic and viscoelastic media and its energetics. WIAS Preprint 1285, Weierstrass Institute for Applied Analysis and Stochastics, Berlin.

Ortiz, M. and Simo, J. C. (1986). An analysis of a new class of integration algorithms for elastoplastic constitutive relations. *International Journal for Numerical Methods in Engineering*, 23(3):353–366.

Rektorys, K. (1982). *The method of discretization in time and partial differential equations*. Mathematics and its Applications. D. Reidel Publishing Company, Dordrecht, Holland.

Roubíček, T. (2005). *Nonlinear partial differential equations with applications*, volume 153 of *International Series of Numerical Mathematics*. Birkhäuser Basel.

Rypl, D. (1998). *Sequential and parallel generation of unstructured 3D meshes*, volume 2 of *CTU Reports*. Czech Technical University in Prague.